Kinetic Simulation Study of Magnetized Collisionless Shock Formation on a Terawatt Laser System

Y. Zhang,[1,2] J. R. Davies,[1,2] P. V. Heuer,[1] and C. Ren[1,2,3]

[1]Laboratory for Laser Energetics, University of Rochester
[2]Department of Mechanical Engineering, University of Rochester
[3]Department of Physics and Astronomy, University of Rochester

In the cosmos, magnetized collisionless shocks such as termination shocks and bow shocks are ubiquitous. These shocks are usually magnetized by astronomical objects and are believed to be an important source of nonthermal particles in the universe. High-power laser systems are capable of reproducing these conditions in the laboratory and enable the systematic study of the underlying physics. It is well known that collisionality is very low due to low plasma density in space; collisions therefore cannot provide efficient dissipation for the shock. A modified two-stream instability (MTSI) has been proposed as the main dissipation mechanism for (quasi-) perpendicular collisionless shocks.[1,2] Previous kinetic particle-in-cell (PIC) simulations used reduced ion–electron mass ratio, an unrealistic high magnetic field, or reduced speed of light to save computational resources; these concessions may alter the relative importance of different physical processes. In this summary our simulations use realistic and experimentally accessible parameters to capture true physics and provide a direct reference for experiments.

In the experimental setup shown in Fig. 1(a), a laser-driven solid-density piston is launched to drive a collisionless shock in a premagnetized ambient hydrogen or neon plasma. The external magnetic field is applied by MIFEDS (magneto-inertial fusion electrical discharge system).[3] In the simulations, as seen in Fig. 1(b), the piston is idealized by a fixed reflecting wall on the right boundary. The ambient plasma drifts toward the wall, which leads to a clear shock downstream free of the influence from the piston. This drifing velocity V_d in the simulation frame is identical to the piston velocity V_p in the lab frame.

To create a collisionless shock the ion collisional mean free path between piston ions and ambient ions must be much larger than the shock width L, and the piston velocity must be supermagnetosonic. These two conditions constrain the ambient plasma density,

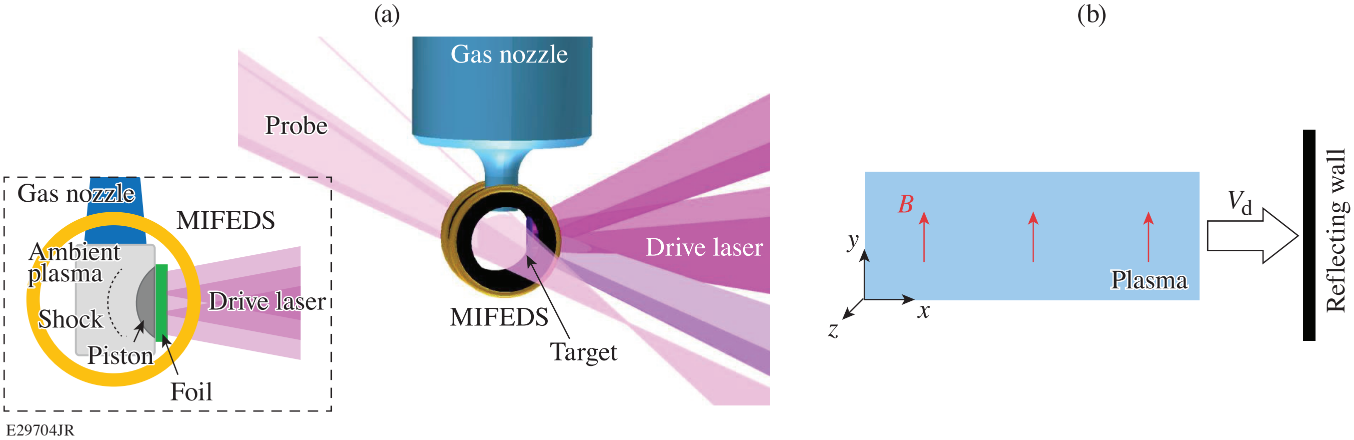

Figure 1
(a) Experimental setup and top-down schematic; (b) reflecting wall simulation setup.

$$\frac{27Z_\mathrm{i}\left(\frac{B_1^T}{50}\right)^2}{56\frac{m_\mathrm{i}}{m_\mathrm{H}}\left(\frac{V_\mathrm{p}^{\mathrm{km/s}}}{500}\right)^2 - Z_\mathrm{i}\frac{T_\mathrm{e1}^\mathrm{eV}}{50} - \frac{T_\mathrm{i1}^\mathrm{eV}}{50}} < n_\mathrm{e1}^{10^{19}\mathrm{cm}^{-3}} \ll \frac{131}{\ln\Lambda}\left(\frac{m_\mathrm{i}}{m_\mathrm{H}}\right)^2\frac{1}{Z_\mathrm{i}^3}\left(\frac{L^{\mu\mathrm{m}}}{100}\right)^{-1}\left(\frac{V_\mathrm{p}^{\mathrm{km/s}}}{500}\right)^4, \tag{1}$$

where m, n, Z are the particle mass, density, charge number, respectively; B is the magnetic field; V_p is the piston velocity; subscripts i, H, and e denote ion, proton, and electron, respectively; 1 (2) represents the upstream (downstream) direction; and the superscripts indicate the units of the parameters.

The growth of MTSI has been used to find suitable parameter space for OMEGA EP[4] experiments. The dispersion relation of MTSI is written as[5]

$$1 + \frac{\omega_\mathrm{pe}^2}{k^2 v_\mathrm{the}^2}\left[1 - \exp(-\lambda_\mathrm{e})\sum_{m=-\infty}^{\infty} I_\mathrm{m}(\lambda_\mathrm{e})\frac{\omega}{\omega + m\Omega_\mathrm{ce}}\right] - \sum_{s=\mathrm{in,re}}\frac{\omega_\mathrm{ps}^2}{2k^2 v_\mathrm{the}^2} Z'(\xi_\mathrm{s}) = 0, \tag{2}$$

where ω_ps is the plasma frequency for species s (e for electrons, in for incoming ions, and re for reflected ions), $v_\mathrm{ths} = (T_\mathrm{s}/m_\mathrm{s})^{1/2}$ is the thermal velocity, Ω_cs is the gyrofrequency, k is the mode number, $\lambda_\mathrm{e} = k^2 v_\mathrm{the}^2/\Omega_\mathrm{ce}^2$, I_m is the modified Bessel function of the first kind, Z is the plasma dispersion function, and $\xi_\mathrm{s} = (\omega - kV_\mathrm{xs})/\sqrt{2}kv_\mathrm{ths}$, where v_xs is the bulk velocity of the two ion species. Equation (2) can be solved numerically for $\omega = \omega_\mathrm{r} + i\omega_\mathrm{i}$, from which the maximum growth rate $\gamma_\mathrm{MTSI} = [\omega_\mathrm{i}]_\mathrm{max}$, and the corresponding, most-unstable mode k_MTSI, and wavelength $\lambda_\mathrm{MTSI} \equiv 2\pi/k_\mathrm{MTSI}$ can be found. Under zero-current condition and the assumptions $n_\mathrm{in}/n_\mathrm{re} = 3$, $V_\mathrm{in} = V_\mathrm{d}/4$, $V_\mathrm{re} = 3V_\mathrm{d}/4$, it is found that the maximum growth rate of MTSI is much larger than the ion gyrofrequency when $M_\mathrm{s1} \geq 4$ for hydrogen and $M_\mathrm{s1} \geq 2$ for neon, indicating a shock can be readily formed within a few tenths of an ion gyration period. Alternately, with an achievable applied magnetic field of only tens of tesla, it is possible to create a shock within a few tenths of a nanosecond. Typical parameter ranges achievable on the OMEGA EP/MIFEDS platform are given in Table I. Based on the conditions discussed in this section we chose upstream parameters listed in Table I for our PIC simulations to study shock formation in more detail. The MTSI, collisionality parameters, and some dimensionless quantities are also shown in Table I.

Hydrogen and neon shocks both form within $\sim\gamma_\mathrm{MTSI}^{-1}$. Figure 2 shows the hydrogen shock as an example. At t = 0.126 ns ($\approx$ 0.10 $T_\mathrm{ci1} \approx 1.1/\gamma_\mathrm{MTSI}$), a shock with a compression ratio of $r \approx 2.35$ [Fig. 2(a)] is formed by the $M_\mathrm{sp} = 3.5$ ideal piston. The presence of reflected ions [the density hump in the upstream region in Fig. 2(a) and the lower prong of the tuning fork structure in Fig. 2(b)] indicates the supercriticality of the formed shock. MTSI is induced by the interaction between the incoming ion and shock-reflected ion in the background magnetic field. Nonzero modes in the Fourier spectrum of E_x [modes 1 and 2 in Fig. 2(c)] further confirm MTSI is the operating instability, in good agreement with the solutions of the dispersion relation.

The reflected ions are accelerated in both shock normal and tangential directions by the electrostatic field and the motional electric field, respectively, to 6.6 to 9.7 keV (average ~8 keV) in the lab frame. These ions accumulate in the upstream and participate in shock-front reformation (on the time scale of a few Ω_ci^{-1}) in later times. Our results using realistic parameters substantially separate the shock-formation time from Ω_ci^{-1} versus previous simulations using reduced $m_\mathrm{i}/m_\mathrm{e}$, showing that these shocks are formed via MTSI. Electrons are heated isotropically to $T_\mathrm{e2} \approx 200$ eV. Additional 1-D simulations further confirm that the shock is indeed collisionless and the reflecting wall is a good approximation of a realistic piston. The formed shocks are also well described by Rankine–Hugoniot jump conditions.

This material is based upon work supported by the Department of Energy National Nuclear Security Administration under Award No. DE-NA0003856, Department of Energy Award No. DE-SC0020431, and the resources of the National Energy Research Scientific Computing Center (NERSC), a U.S. Department of Energy Office of Science User Facility located at Lawrence Berkeley National Laboratory. The authors thank the UCLA-IST OSIRIS consortium for the use of OSIRIS.

Table I: Parameters for the OMEGA EP/MIFEDS platform and the hydrogen/neon simulations, with corresponding MTSI growth rate/mode number of the most-unstable mode and some key dimensionless quantities. The plasma beta is $\beta = 2\mu_0(n_i T_i + n_e T_e)/B^2$, $\tau = \omega_{pe}^2/\Omega_{ce}^2$ is the magnetization parameter. The piston velocity range is from *HYDRA*[6] simulations of the proposed experimental setup.

		OMEGA EP/MIFEDS	Hydrogen	Neon (Ne^{8+})
Upstream				
Density	n_{e1}	10^{18} to 10^{20} cm^{-3}	10^{19} cm^{-3}	6×10^{18} cm^{-3}
Temperature	T_1	40 to 400 eV	50 eV	160 eV
B field	B_1	$\leq$50 T	50 T	50 T
Piston velocity	V_p	$\leq$500 km/s	442 km/s	375 km/s
Ion gyroradius	ρ_{i1}		92.3 μm	195.7 μm
Ion gyroperiod	T_{ci1}		1.3 ns	3.3 ns
MTSI				
Maximum growth rate	γ_{MTSI}		8.8 ns^{-1}	6.7 ns^{-1}
Most-unstable mode	λ_{MTSI}		10.7 μm	14.2 μm
Dimensionless				
Piston sonic Mach number	M_{sp}		3.50	3.50
Alfvénic Mach number	M_{Ap}		1.28	1.33
Magnetosonic Mach number	M_{msp}		1.20	1.25
Ion mean free path	$\lambda_{ii}/\lambda_{MTSI}$		74	40
MTSI growth rate	$\gamma_{MTSI}/\Omega_{ci1}$		11.5	21.9
Plasma beta	β_1		0.16	0.17
Magnetization	τ_1		421	247

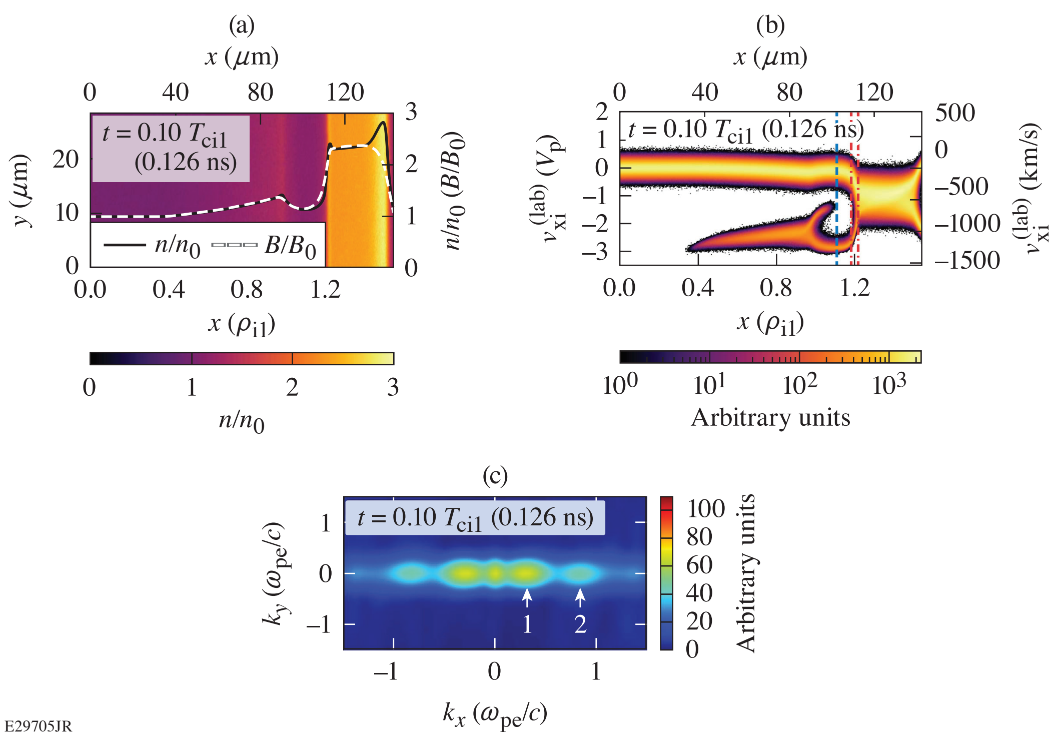

Figure 2
(a) Hydrogen ion density (2-D and y averaged) and magnetic field (y averaged) at $t = 0.10\ T_{ci1}$; (b) Ion v_{xi}–x phase space in the lab frame; (c) Fourier spectrum of E_x. The modes labeled with 1 and 2 are $k_x \approx 0.33$ and $0.86\ \omega_{pe}/c$, respectively.

1. J. Park *et al*., Phys. Plasmas **19**, 062904 (2012).
2. J. Park *et al*., Astrophys. J. **765**, 147 (2013).
3. D. H. Barnak *et al*., Rev. Sci. Instrum. **89**, 033501 (2018).
4. D. N. Maywar *et al*., J. Phys.: Conf. Ser. **112**, 032007 (2008).
5. S. P. Gary, *Theory of Space Plasma Microinstabilities*, Cambridge Atmospheric and Space Science Series (Cambridge University Press, Cambridge, 1993).
6. M. M. Marinak *et al*., Phys. Plasmas **8**, 2275 (2001).